GaSb Quantum-Rings for Vertical-Cavity Surface-Emitting Lasers Emitting at Telecommunications and Mobile Sensing Wavelengths

S. O. Jones, P. D. Hodgson, M. Hayne
Lancaster University, Bailrigg, Lancaster, Lancashire, LA1 4YW, United Kingdom

ABSTRACT

Renewed interest in vertical-cavity surface-emitting lasers (VCSELs) operating in the regions of 1300 and 1550 nm has come as a result of the desire for so-called 'eye-safe' lasers (>1400 nm) in consumer applications, for below-screen sensing in mobile devices (>1380 nm) and for light detection and ranging (LiDAR). Current VCSELs have a host of applications, including printing, bar code reading, data communications and facial recognition systems. Typical (In)GaAs quantum-well VCSEL active-regions are sub-optimal for reaching telecoms and 'eye-safe' wavelengths because of the large strain accompanying the increased In fraction required. Here, a case is made for the use of GaSb quantum rings (QRs) over other materials in VCSEL active regions for devices across the telecoms range. The design and fabrication of two prototype quantum ring VCSELs is discussed and provisional results are presented for continuous operation at room temperature and at 77 K. The origin of background emission is considered and a sub-milliamp threshold current achieved for emission at 1257 nm.

Keywords: GaSb quantum rings, vertical-cavity surface-emitting lasers (VCSELs), emission properties, laser, telecoms, molecular beam epitaxy (MBE), quenching

1. INTRODUCTION

GaSb quantum rings represent an interesting contender for the active (light-emitting) entities in vertical-cavity surface-emitting lasers (VCSELs) targeting applications from 1100 nm to 1600 nm. Existing VCSEL technologies are ubiquitous in a variety of applications, including data communications and facial recognition systems operating at <1000 nm[1]. Although they have taken over in many markets, VCSELs are yet to play a significant role in applications requiring 1300 to 1550 nm emission. A key factor preventing the expansion of the VCSEL industry into longer-wavelength applications is the lattice mismatch and resulting strain between GaAs substrates or distributed Bragg reflectors (DBRs) and InGaAs quantum-well active regions with sufficient indium to reach those longer wavelengths. Below-screen sensing in mobile devices (>1380 nm) and so-called 'eye-safe' lasers (>1400 nm) for light detection and ranging (LiDAR) applications are driving the desire for low-cost, high-efficiency VCSELs at the extended wavelengths, driving alternative approaches such as dilute-nitride VCSELs[2].

GaSb quantum rings (QRs) are zero-dimensional type-II nanostructures capable of emitting across a broad spectrum, including the telecoms O-band and C-band. The full range of the quantum ring emission is represented by the photoluminescence (PL) emission shown in figure 1. A broad gain spectrum is typically seen as detrimental to a laser. In the case of a VCSEL, the lasing wavelength is determined by the cavity length and can be selected by changing the cavity thickness and DBR stopband position. This results in a narrow emission line and rejection of other wavelengths, including those contained within the gain spectrum of the active region. The type-II nature of the rings is similarly also conventionally seen as detrimental to the performance of a laser due to long recombination lifetimes[3]. However, this is mitigated by the strong enhancement of the recombination rate at the cavity. The rings are grown monolithically by molecular beam epitaxy (MBE) on GaAs through a strain-releasing process and are compatible with the favored GaAs/$Al_xGa_{1-x}As$-DBR technology. Furthermore, in contrast to quantum dots where the linewidth broadening is attributed to inhomogeneity in the size of the dots and the subsequent perturbation of the energy levels[4], the broad emission of the quantum-rings is attributed to capacitive charging effects[5]. This suggests that the emission wavelength of each QR is largely determined by its charge state (hole occupancy), allowing it to emit across the gain spectrum simply by adding or removing charge, and potentially reduces the gain limitation in quantum dot lasers that is attributed to inhomogeneous growth and fewer dots taking part in the emission. The authors thus propose the use of GaSb QRs as the active region in VCSELs for telecoms and mobile device applications such as below-screen, time-of-flight facial

recognition systems. Such devices take advantage of the long spontaneous emission times characteristic of type-II QRs for reduced background and enable stimulated emission at wavelengths across the telecoms band through cavity and DBR design. In this work, a discussion of the device design and fabrication will be followed by the latest results for 77 K and room-temperature operation.

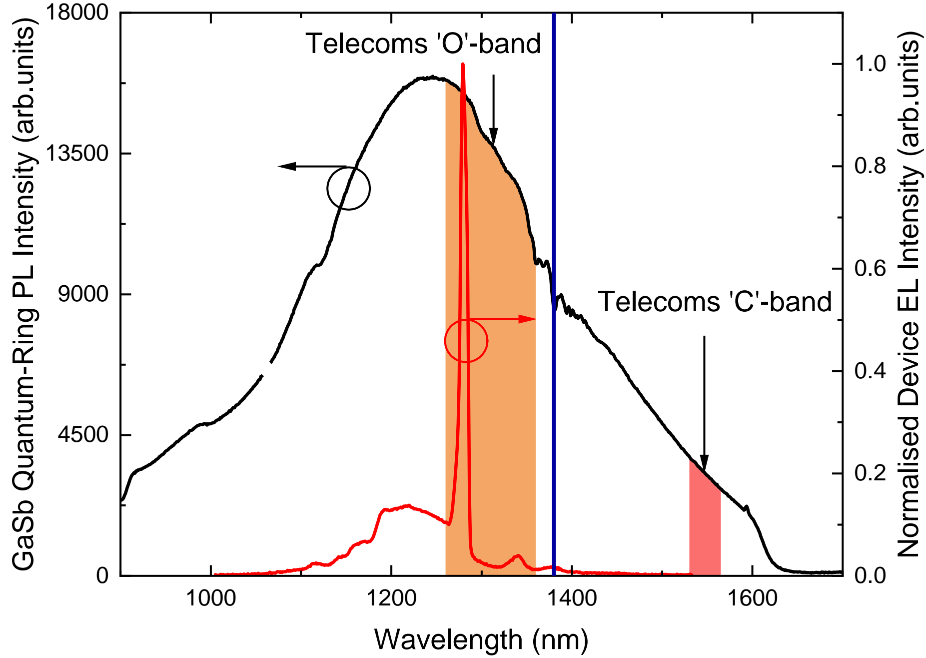

Figure 1. Room temperature photoluminescence (PL) of GaSb quantum rings with comparison to electroluminescence (EL) for GaSb QR VCSEL material. The telecoms ‘C’-band and ‘O’-band are indicated by the shaded regions whilst the lower cutoff for below screen applications is indicated by the blue vertical line.

2. DEVICE DESIGN AND FABRICATION

Similar structures were produced for GaSb QR VCSELs, with cavity lengths of $\lambda/2$ and $3\lambda/2$. Both structures utilize a GaAs cavity containing five QR layers nominally centered around the antinodes of the electric field in the cavity, with the expectation that the greater number of QR layers in the $3\lambda/2$ cavity would allow for more intense output without saturating the recombination rate of rings at the wavelength corresponding to the cavity resonance. The DBRs consist of thirty-four repeats of Si-doped GaAs/$Al_{0.9}Ga_{0.1}As$ for the lower n-type DBR and twenty-one Be-doped repeats for the p-type upper. Both include a 15 nm intermediate composition ($Al_{0.6}Ga_{0.4}As$) layer at the interface between GaAs/$Al_{0.9}Ga_{0.1}As$ to reduce the electrical resistance caused by barriers formed by band bending at the interfaces[6]. The DBR stopband was designed with a center at 1270 nm to meet XGS-PON fiber-to-the-home wavelength requirements. $Al_{0.6}Ga_{0.4}As$ spacer layers were used to tune the cavity response to reach the 1270 nm target (fig. 2.). The full structure for the $3\lambda/2$ cavity can be seen in figure 3 and includes an additional high Al-content layer compatible with wet oxidation which was not present in the shorter cavity.

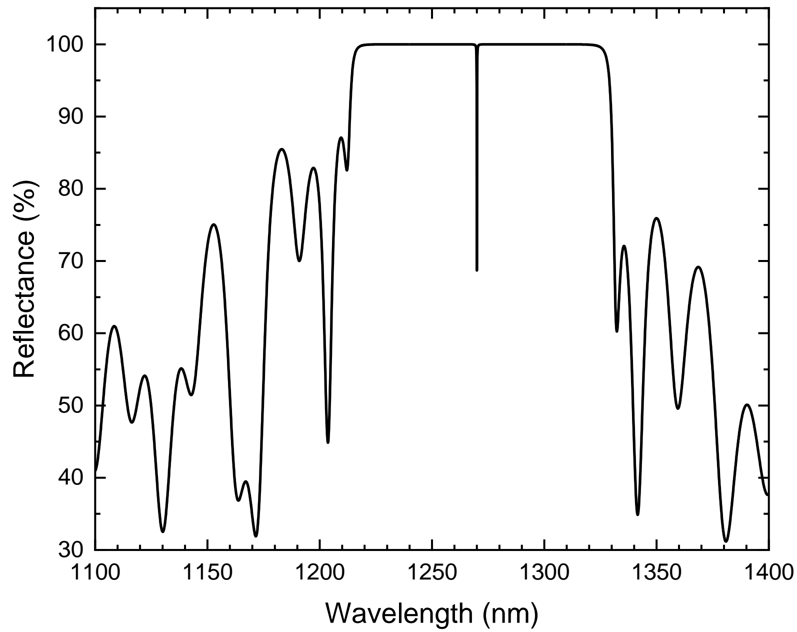

Figure 2. Reflectance for 3λ/2 GaSb QR VCSEL simulated using the software TFCalc, with a cavity resonance at 1270 nm.

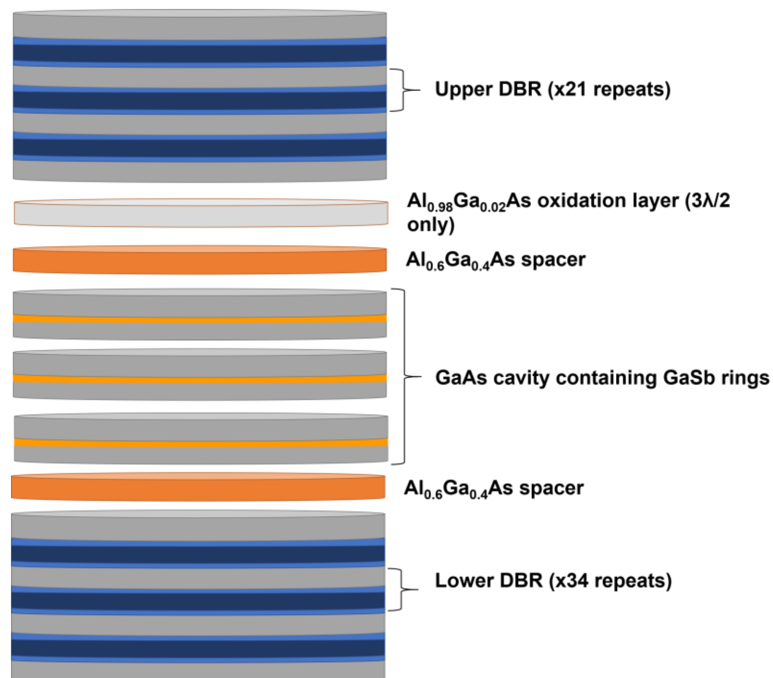

Figure 3. Schematic of a GaSb QR VCSEL layer structure with a 3λ/2 cavity. $GaAs/Al_{0.6}Ga_{0.4}As/Al_{0.9}Ga_{0.1}As$ step-graded DBRs surround a GaAs-cavity containing sets of five quantum rings centered around each maximum in electric field intensity.

The structures were grown by molecular beam epitaxy (MBE) on a Veeco GENxplor MBE system. The QRs are deposited as quantum dots, produced using the Stranski-Krastanow method, before a carefully controlled cold-cap GaAs layer is grown on top, during which As-Sb exchange results in the formation of the rings in a strain-reducing process (fig. 4).

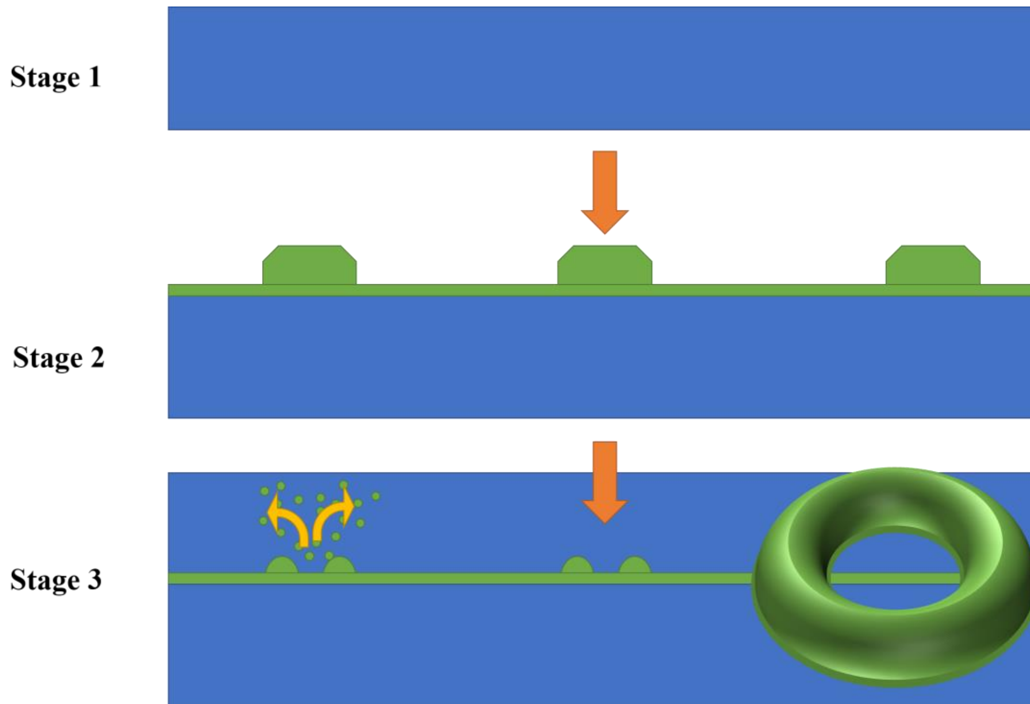

Figure 4. An artistic interpretation of the cross-section for growth of GaSb quantum dots on GaAs by the Stranski-Krastanow (SK) method before capping with a carefully controlled GaAs layer results in the formation of rings through As-Sb exchange. Stage 1 represents a GaAs surface, upon which the wetting layer and SK GaSb QDs are grown (stage 2). The final stage involves the growth of a cold-cap GaAs layer (upper blue layer in stage 3) and As-Sb exchange which results in the ring geometry. The final cross-section indicates the lobes of a cross-sectioned ring.

Fabrication of the VCSEL devices consists of a multi-step process. First, Au/Ni/Au contacts are deposited on the p-type GaAs surface. Plasma-enhanced chemical-vapor deposition (PECVD) is used to deposit Si_3N_4 on the surface of the sample to provide electrical isolation of the bond pads and epi-surface. Reactive-ion etching (RIE) is then used to open a window in the isolation layer above the contacts and device emission surface before the TiAu bond pads are deposited. A bridge-style device geometry (fig. 5) is used to avoid the requirement for planarization after etching of the device mesa, and therefore simplifies the process. A combination of RIE to remove the nitride passivation and chlorine-based inductively-coupled plasma (ICP) etching to etch the III-V material is used to form the device mesas by etching into the top repeat of the lower DBR, using laser-reflectometry techniques to determine the appropriate endpoint. A second Si_3N_4 layer is employed to passivate the device and ensure stability outside of the cleanroom environment. Access to the bond pads and emission windows is regained in an RIE etch before the backside AuGe/Ni/Au contact is deposited. A final rapid thermal annealing process is used to ensure ohmic contacts between the GaAs tri-layer metal stacks. Individual devices are cleaved and bonded onto TO46 headers for testing in a dedicated optical setup. A diagram of the process flow can be seen in figure 5.

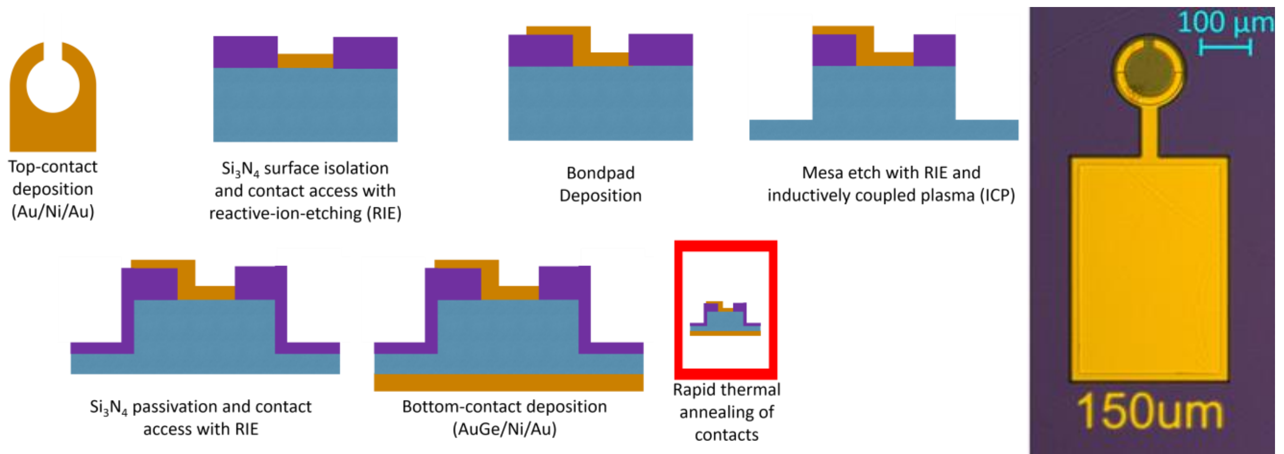

Figure 5. The process flow for fabrication of GaSb QR prototype devices consists of top-side metallization, surface isolation and regaining of access to the top contact and emission window. Bond pads are deposited on the planar structure before the mesa-defining etch. Environmental passivation with Si_3N_4 is performed before regaining access to the bond pads and emission windows. The backside contact is deposited before rapid thermal annealing is used to ensure ohmic-contact to both the top-surface and backside. On the right hand side is an optical microscope image of the GaSb QR VCSEL.

3. RESULTS AND DISCUSSION

3.1 Room temperature

A temperature sweep from 20°C (room temperature) to 60°C exhibits the characteristic redshift of emission wavelength which is well known for VCSELs, due changes in the refractive index and thus cavity resonance. In this instance, it is notable that the background emission across the quantum ring spectrum appears to be suppressed compared to the cavity peak when temperature increases, as seen when plotted on a normalized scale (fig. 6). The authors suspect that the reduction in background is due to non-radiative recombination being favored over the slow spontaneous recombination, whereas the cavity-enhanced peak emission wavelength, which has a significantly reduced recombination time, is less affected.

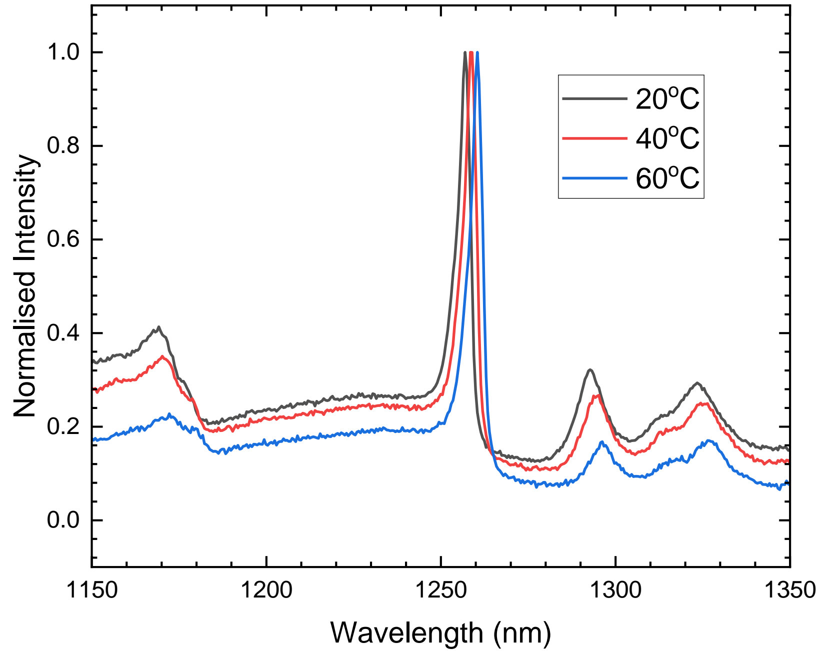

Figure 6. Sweeping temperature from 20°C to 60°C exhibits a redshift in emission wavelength for a 3λ/2 cavity structure with 30 µm mesa diameter, typical of VCSEL devices. When compared on a normalized scale it is notable that the background emission is suppressed relative to the cavity resonance.

It was speculated that the stimulated emission for a λ/2 cavity would be limited by the number of QRs emitting at that wavelength and the maximum recombination rate of the rings, leading to a larger background due to spontaneous recombination of carriers at wavelengths not enhanced by the cavity. Therefore, the 3λ/2 cavity structure was grown to allow for more QR layers, with the expectation of a reduced background and comparatively more emission at the resonant wavelength than the λ/2 structure. Room-temperature measurements of both structures are shown in figure 7. In fact, both structures show prominent peaks at the cavity resonance and a significant background. It should be noted that both structures were designed to emit at 1270 nm but did not hit the target due to layer thicknesses varying as a result of growth rates deviating from the calibrations. Given that the relative intensity of the background compared to the cavity peak in the 3λ/2 structure is increased, which is the opposite our expectation, we now suspect that the broad background emission is a result of spontaneous recombination in quantum rings located (inadvertently) further from the antinodes of the electric field. Work to investigate this hypothesis is currently in progress: transmission-electron microscopy will be used to determine the position of the rings within the cavity and the extracted layer thicknesses will be used to simulate the electric field antinodes for the sample as-grown.

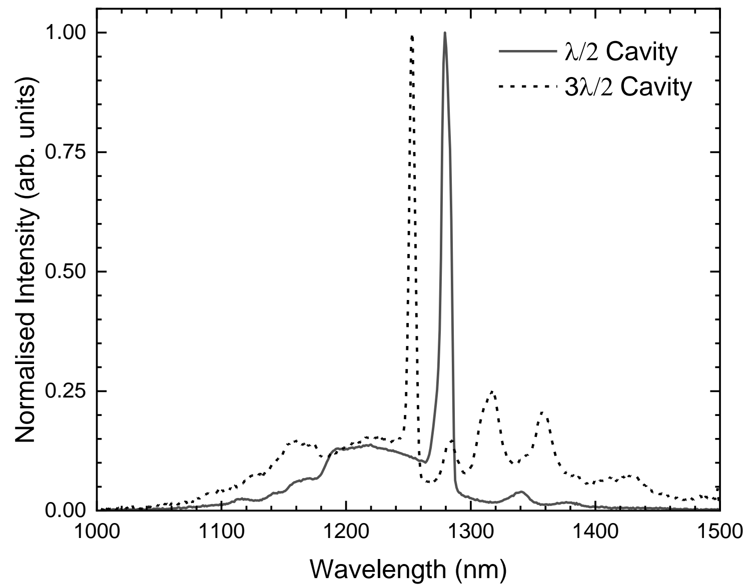

Figure 7. Room-temperature emission for GaSb QR VCSELs shows a sharp emission peak at the cavity resonance. Both structures were designed for operation at 1270 nm but deviate due to deviation from the design which is a result of growth rate deviating from the initial calibrations.

Voltage-current and intensity-current measurements at the cavity resonance (1257 nm for this sample) are shown for continuous room-temperature operation of a 3λ/2 cavity GaSb VCSEL with 10 µm mesa diameter (fig. 8 left). A clear laser-like threshold is visible in the intensity-current characteristic at the peak wavelength of the structure, and is identified to be in the region of 0.115 mA by taking the second derivative of the normalized light intensity with respect to current (fig. 8 right), corresponding to a very low threshold current density of approximately 0.15kA/cm^2 for the 10 µm mesa.

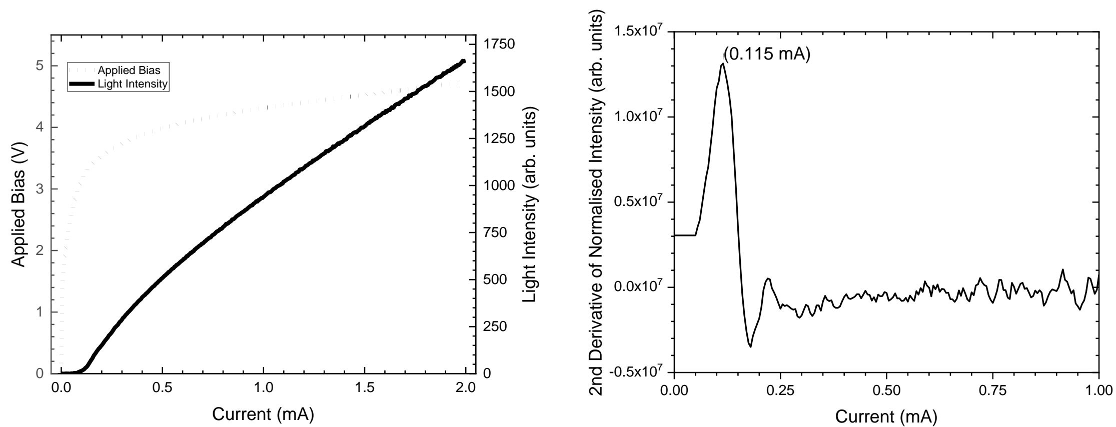

Figure 8. Room-temperature (20°C) voltage-current and intensity-current measurements for continuous operation of a GaSb quantum-ring VCSEL with 10 µm mesa at 1257 nm (left). Threshold current for continuous room-temperature (20°C) operation of a GaSb quantum-ring VCSEL with 10 µm mesa is indicated at the maximum of the second derivative of the output intensity with respect to current (right).

3.2 77 K measurements

At 77 K the emission of the VCSEL is blue shifted relative to room-temperature as expected (fig. 9). The background emission is also blue-shifted, as expected due to an increase in bandgap[3], and more intense relative to the room temperature data. The explanation for the increased intensity of the background is analogous to the explanation given for the room-temperature to 60°C sweep discussed in section 3.1, i.e., at lower temperatures the non-radiative recombination is reduced and therefore does not suppress the slower, spontaneous recombination.

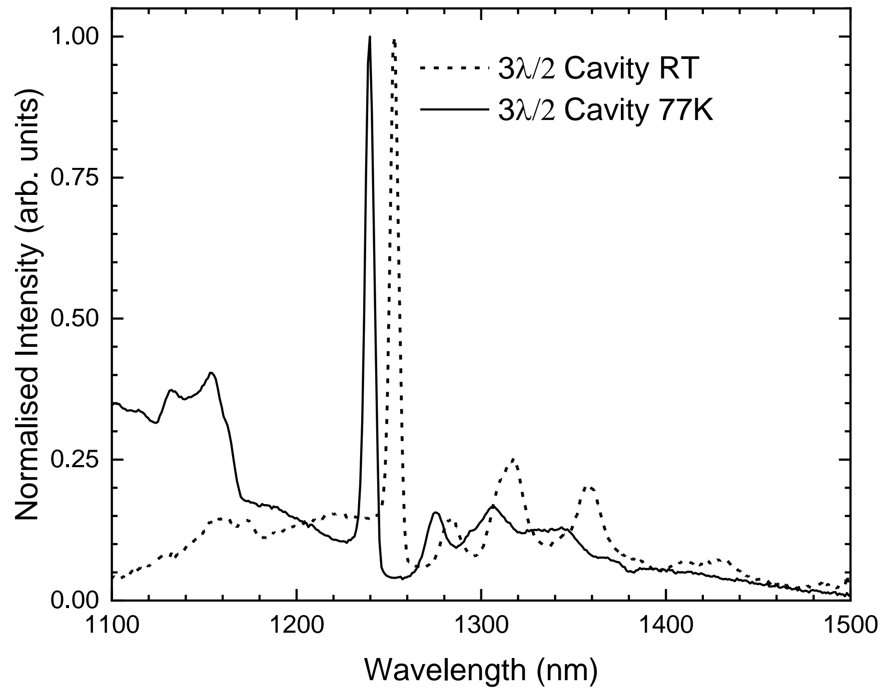

Figure 9. Room-temperature and 77K spectra of a GaSb quantum-ring VCSEL with 30 μm mesa operating continuously at 1.5 mA.

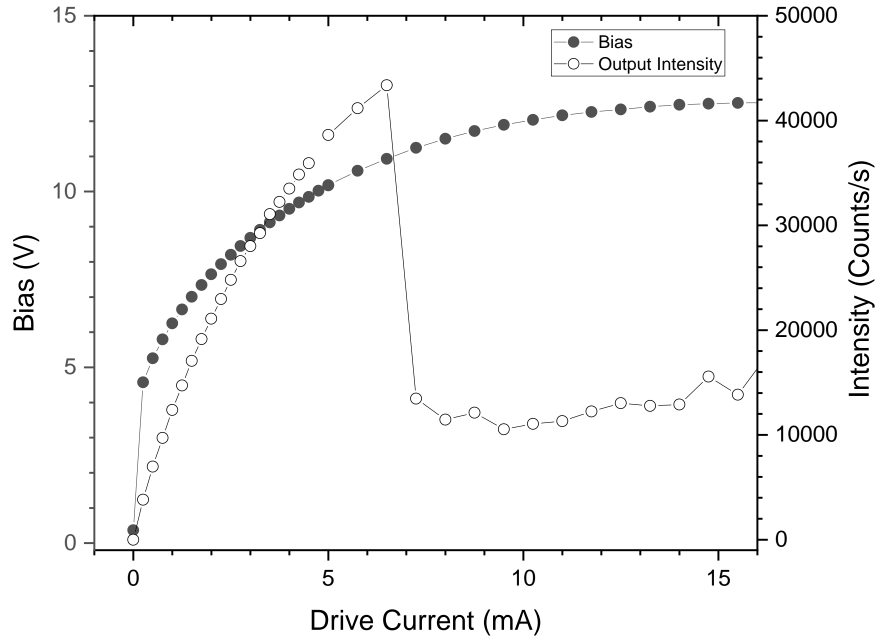

Figure 10. Voltage-current and intensity-current measurements for a 3λ/2 GaSb quantum-ring VCSEL with 30 μm mesa operating with a peak wavelength of 1240 nm at 77K. A distinct drop in output intensity is apparent in the region of 6 to 7 mA.

Figure 10 shows the voltage-current and intensity-current measurements for a 3λ/2 cavity VCSEL at 77K. A sharp drop in output intensity is observed at between 5 and 6 mA. It is believed that at this point the electric field is large enough for carriers to overcome the potential barriers present at lower voltages and are swept out of the active region. This results in recombination elsewhere in the structure through both radiative and non-radiative means, reducing radiative contributions from the QRs themselves. The reduction of intensity is visible when comparing the 5 mA and 8 mA sweeps (fig. 11 left). In particular, the reduction in intensity is much more significant for emission at the resonant cavity wavelength, which is made clear by the large ratio shown in fig 11 (right). At this time, it is unclear what mechanism causes such quenching of the cavity enhancement, but since the cavity peak is quenched much more than the background spontaneous emission, it seems that the amplification within the device is suppressed.

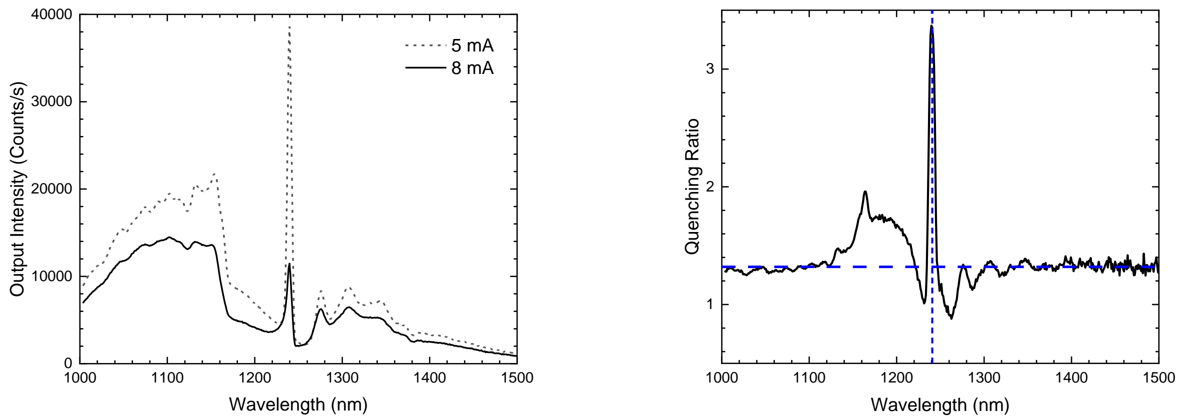

Figure 11. Emission spectra for a GaSb quantum-ring VCSEL with 30 µm mesa operating continuously at 77K for 5 mA and 8 mA (left). It is notable that the 8 mA drive current corresponds to a lower output intensity, contrary to expectations. On the right, the ratio of 5 mA drive current intensity to 8 mA drive current intensity which shows a stark quenching of the cavity enhanced emission. Horizontal and vertical dashed lines have been added to guide the eye.

4. CONCLUSIONS

The design and fabrication process were presented for QR-based VCSELs targeting the XGS-PON fiber-to-the-home (FTTH) upstream wavelength. The devices showed a strong cavity response, but with large background emission which decreases relative to the cavity resonance at elevated temperatures. Spontaneous emission from QRs located away from electric field antinodes may contribute significantly to the background emission. This could be reduced using fewer QR layers positioned directly on the electric field antinodes. Intensity-current measurements at the peak emission wavelength showed laser-like threshold current characteristics with sub-milliamp threshold current. Strong suppression of the cavity-enhanced emission at large biases, observed at 77 K, indicates the quenching of amplification by stimulated emission of radiation, and accompanies an overall reduction in intensity resulting from carriers leaking through the VCSEL cavity. In summary, these provisional results show promise for VCSEL emission across the range of wavelengths supported by the quantum rings, and may find applications in ‘eye-safe’ LiDAR, mobile sensing and FTTH.

5. ACKNOWLEDGEMENTS

This work was supported by an EPSRC ICASE studentship (EP/T517392/1) with IQE plc, and by the 2017–2020 Impact Acceleration Account funding allocation to Lancaster University under grant EP/R511560/1.

REFERENCES

[1] Liu, A., et al., “Vertical-cavity surface-emitting lasers for data communication and sensing,” Photonics Research, 7(2), 121-136 (2019).
[2] Gebski. M., et al., “Baseline 1300 nm dilute nitride VCSELs,” OSA Continuum, 3(7), 1952-1957 (2020).
[3] Hodgson, P.. et al., “GaSb quantum rings in GaAs/$Al_xGa_{1-x}As$ quantum wells,” J. Appl. Phys. 119(4), 044305 (2016).
[4] O. Qasaimeh, "Effect of inhomogeneous line broadening on gain and differential gain of quantum dot lasers," IEEE Transactions on Electron Devices, vol. 50, no. 7, 1575-1581 (2003)

[5] Hodgson, P.. et al., "Blueshifts of the emission energy in type-II quantum dot and quantum ring nanostructures," J. Appl. Phys. 114(7), 073519 (2013).
[6] T. E. Sale, "Vertical cavity surface emitting lasers," University of Sheffield (1993).